Available online at www.sciencedirect.com

ScienceDirect

Computational Materials Science 42 (2008) 614–618

COMPUTATIONAL MATERIALS SCIENCE

www.elsevier.com/locate/commatsci

First-principles study of structural, elastic, electronic, and optical properties of orthorhombic $BiGaO_3$

Chenliang Li[a], Biao Wang[a,b,*], Rui Wang[c], Hai Wang[a], Xiaoyan Lu[a]

[a] School of Astronautics, Harbin Institute of Technology, Harbin, China
[b] School of Physics Science and Engineering, Sun Yat-sen University, Guangzhou, China
[c] Department of Applied Chemistry, Harbin Institute of Technology, Harbin, China

Received 20 August 2007; received in revised form 19 September 2007; accepted 24 September 2007
Available online 5 November 2007

Abstract

The structural parameters, elastic, electronic, and optical properties of orthorhombic $BiGaO_3$ were investigated by the density functional theory. The calculated structural parameters are in agreement with previous calculation and experimental data. The structural stability of $BiGaO_3$ has been confirmed by calculations of the elastic constants. The energy band structure, density of states, and Mulliken charge population were obtained. $BiGaO_3$ presents a direct band gap of 2.03 eV. Furthermore, the absorption spectrum, refractive index, extinction coefficient, reflectivity, energy-loss spectrum, and dielectric function were calculated. The origin of the spectral peaks was interpreted based on the electronic structures.

PACS: 71.15.Mb; 73.20.At; 74.25.Gz; 78.20.Ci

Keywords: Density functional theory; Structural properties; Elastic constants; Electronic properties; Optical properties

1. Introduction

$BiMO_3$ compounds, with nonmagnetic elements M (M = Al, Ga, Sc, In), have received a lot of attention because the solid solutions of $BiMO_3$–$PbTiO_3$ can improve ferroelectric properties of $PbTiO_3$ and reduce the amount of lead [1–6]. $BiScO_3$ has been studied using both experimental and theoretical methods [5–7]. It was suggested that $BiScO_3$ could substitute for $PbZrO_3$ in $Pb(Zr,Ti)O_3$ (PZT). In 2005, Baetting et al. [8] theoretically predicted the large ferroelectric polarization and piezoelectricity in the hypothetical perovskite-structure oxides $BiAlO_3$ and $BiGaO_3$. They proposed the $Bi(Al,Ga)O_3$ system as a replacement for the widely used piezoelectric material, PZT, that will avoid the environmental toxicity problems of lead-based compounds. Therefore, the studies on the crystal structures and related physical properties of $BiAlO_3$ and $BiGaO_3$ are of great interest. Belik et al. [9] prepared $BiAlO_3$ and $BiGaO_3$ under high-pressure, high-temperature technique, respectively. It is reported that $BiAlO_3$ is isotypic with multiferroic perovskite-like $BiFeO_3$, while $BiGaO_3$ has the orthorhombic structure closely related to that of the pyroxene-like KVO_3. Furthermore, to understand the origin of ferroelectricity in $BiMO_3$ materials, Wang et al. [10,11] studied the structures, energy bands, and density of states of cubic $BiMO_3$ using the full potential linearized augmented plane wave (FP-LAPW) method. However, the properties of orthorhombic $BiGaO_3$ are not studied theoretically.

In this work, we focus on the structure, elastic constants, electronic, and optical properties of orthorhombic $BiGaO_3$ using the first-principles density function theory. The elastic constants can provide valuable information about the anisotropic character of the bonding and structural stability [12].

---

[*] Corresponding author. Address: School of Astronautics, Harbin Institute of Technology, Harbin, China. Tel./fax: +86 20 84115692.
E-mail address: lichenliang1980@yahoo.com.cn (B. Wang).

0927-0256/$ - see front matter © 2007 Elsevier B.V. All rights reserved.
doi:10.1016/j.commatsci.2007.09.008

2. Computational details

The calculations were performed using the plane-wave pseudopotential method based on density functional theory (DFT). Only valence electrons were taken into account, corresponding to Bi $6s^26p^3$, Ga $3d^{10}4s^24p^1$ and O $2s^22p^4$ electronic configurations, and Ultrasoft Vanderbilt-type pseudopotentials were used [13]. The generalized gradient approximation (GGA) in the scheme of Perdew et al. [14] was used for the exchange and correlation correction. The structural optimizations were conducted using the Broyden–Fletcher–Goldfarb–Shanno minimization (BFGS). Mulliken charges were calculated according to the formalism described by Segall et al. [15]. A plane-wave cutoff energy of 400 eV was employed throughout the calculation. Geometry optimization was achieved using convergence thresholds of 1×10^{-5} eV/atom for total energy, 0.03 eV/Å for maximum force, 0.05 GPa for pressure and 0.001 Å for displacement. The tolerance in the self-consistent field (SCF) calculation is 1.0×10^{-6} eV/atom. For the sampling of the Brillouin zone, the electronic structures and optical properties used a $8 \times 8 \times 6$ and $10 \times 10 \times 8$ k-point grid generated according to the Monkhorst–Pack scheme [16], respectively. The elastic constants were calculated by the 'stress–strain' method.

The optical properties of $BiGaO_3$ is determined by the frequency-dependent dielectric function $\varepsilon(\omega) = \varepsilon_1(\omega) + i\varepsilon_2(\omega)$ that is mainly connected with the electronic structures. The imaginary part $\varepsilon_2(\omega)$ of the dielectric function $\varepsilon(\omega)$ is calculated from the momentum matrix elements between the occupied and unoccupied electronic states and given by

$$\varepsilon_2 = \frac{2e^2\pi}{\Omega\varepsilon_0} \sum_{k,v,c} \left|\langle \psi_k^c | \hat{u} \cdot r | \psi_k^v \rangle\right|^2 \delta(E_k^c - E_k^v - E),$$

where ω is the light frequency, e is the electronic charge, and ψ_k^c and ψ_k^v are the conduction and valence band wavefunctions at $\mathbf{k}$, respectively. The real part $\varepsilon_1(\omega)$ of the dielectric function $\varepsilon(\omega)$ can be derived from the imaginary part $\varepsilon_2(\omega)$ using the Kramers–Kronig dispersion equation. All other optical constants on the energy dependence of the absorption spectrum, the refractive index, the extinction coefficient, the energy-loss spectrum, and the reflectivity can be derived from $\varepsilon_1(\omega)$ and $\varepsilon_2(\omega)$ [17].

3. Results and discussion

3.1. Geometry optimization and elastic constants

$BiGaO_3$ belongs to the space group *Pcca*. There are four $BiGaO_3$ groups (20 atoms) per unit cell. We used X-ray powder diffraction data [9] as a starting point for geometry optimization. We calculated the structural parameters for the orthorhombic and cubic $BiGaO_3$, respectively. The results are summarized in Table 1. For the orthorhombic $BiGaO_3$, the lattice parameters a and b are smaller than the experimental values by 1%, respectively. The lattice parameter c is overestimated 0.5%. These deviations are within the admitted range of the errors of the first-principles method. For the cubic $BiGaO_3$, our results are in agreement with the results that Wang et al. [10] calculated by using an accurate FP-LAPW method. It can be seen that the optimized orthorhombic structure is reasonable. Moreover, it is found that ultrasoft Vanderbilt-type pseudopotentials are appropriate for studying $BiGaO_3$ material.

For orthorhombic crystals, the mechanical stability requires the elastic constants satisfying the well-known Born stability criteria [18]

$$C_{ii} > 0 \quad (i = 1-6), \quad (C_{11} + C_{12} - 2C_{12}) > 0,$$
$$(C_{11} + C_{33} - 2C_{13}) > 0, \quad (C_{22} + C_{33} - 2C_{23}) > 0,$$
$$(C_{11} + C_{22} + C_{33} + C_{12} + 2C_{12} + 2C_{13} + 2C_{23}) > 0.$$

From our calculated C_{ij} shown in Table 2, it is known that the orthorhombic $BiGaO_3$ is mechanically stable. At present, no experimental or theoretical data for the elastic constants of $BiGaO_3$ are available. Therefore, we consider the present results as a prediction study.

3.2. Band structure, density of states and Mulliken charge population

The energy band structure, total density of states, and partial densities of states of $BiGaO_3$ are shown in Figs. 1–3, respectively. The energy band structure is calculated along the way that contains the highest number of high-symmetry points of the Brillouin zone, namely Gamma → $Z \rightarrow T \rightarrow Y \rightarrow S \rightarrow X \rightarrow U \rightarrow R$.

Table 1
The lattice parameters of $BiGaO_3$

	a (Å)	b (Å)	c (Å)	V (Å^3)
$BiGaO_3$				
Orthorhombic				
Calculated[a]	5.360	5.078	9.990	271.92
Experimental[b]	5.416	5.134	9.937	276.29
Cubic				
Calculated[a]	3.834			
FLAPW-GGA[c]	3.816			

[a] This work.
[b] Ref. [9].
[c] Ref. [10].

Table 2
The calculated bulk modulus B_0 (GPa) and elastic constants (GPa) for orthorhombic $BiGaO_3$

$BiGaO_3$			
B_0	129.46	C_{44}	72.35
C_{11}	239.32	C_{55}	46.65
C_{22}	198.18	C_{66}	58.6
C_{33}	165.21	C_{23}	100.7
C_{12}	101.04	C_{13}	93.12

The top of the valence band (VB) and the bottom of the conduction band (CB) are composed of O 2p states and Bi 6p states, respectively. In contrast, the band gap of $PbTiO_3$ ($PbZrO_3$) is determined by O 2p states and Ti 3d (Zr 4d) states rather than those associated with Pb–O. $BiGaO_3$ presents a direct band gap of 2.03 eV at the *X*-point. The band gaps predicted by DFT are smaller than experimental data, which means that our result underestimate the real band gap of $BiGaO_3$. In our calculation, the scissors operator (SO) on both the electronic structure and the optical properties were not considered. The energy bands between −20 and −17 eV mainly consist of O 2s states. The energy bands at about −13 eV consist of Ga 3d states showed a sharp peak due to its strong localization character. The Bi 6s states were located at about −10 eV. By analyzing partial density of states, it was found that the O 2p states have some admixture with the Bi and Ga sp states. Thus, $BiGaO_3$ appears to have some covalent features. Moreover, in the region of the valence band, the width of the PDOS of Bi was clearly narrower than that of Ga and O. The number of peaks was also less than those for Ga. This indicates that the hybridization of Ga–O is stronger than that for Bi–O. Above 3 eV and up to 10 eV, the energy bands derived from the Ga 4p and 4s states force Bi 6p states to move towards the Fermi level. Based on the foregoing results, it is clear that the electronic properties of $BiGaO_3$ are affected by the Ga ion through their influence on the Bi–O bonding.

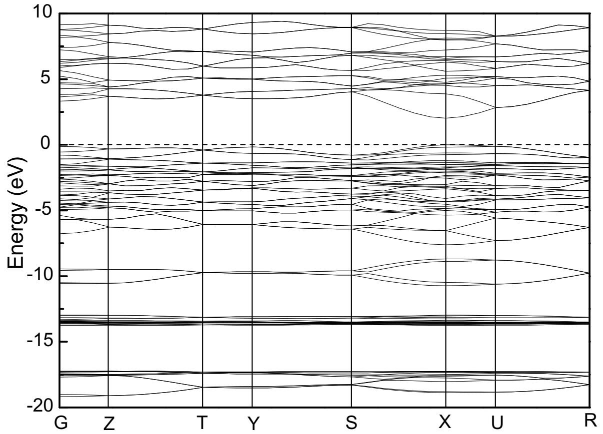

Fig. 1. Calculated energy band structure of orthorhombic $BiGaO_3$.

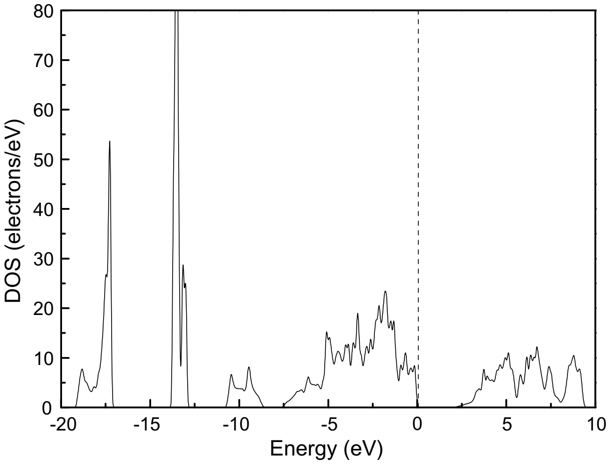

Fig. 2. Calculated total density of states of orthorhombic $BiGaO_3$.

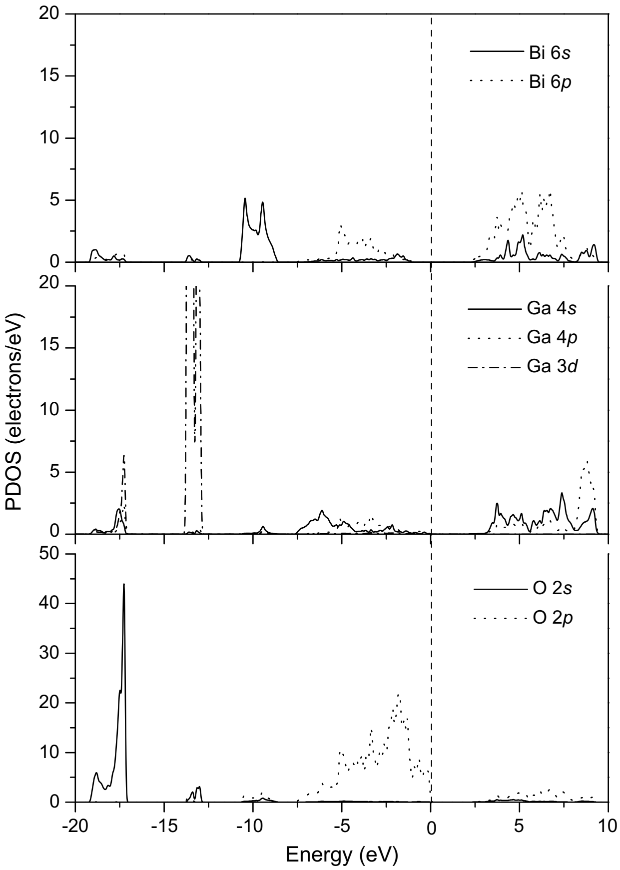

Fig. 3. Calculated partial density of states of orthorhombic $BiGaO_3$.

We also performed the Mulliken charge population for $BiGaO_3$ because it is a good method to understand bonding behavior. The Mulliken population results are given in Table 3. The charge transfer from Bi and Ga to O are about 1.62, 1.16 electrons, respectively. Therefore, we concluded that the bonding behavior of $BiGaO_3$ is a combination of covalent and ionic nature. Moreover, the Ga–O bond possessed a stronger covalent bonding strength than the Bi–O bond. The results are consistent with our DOS calculation.

Table 3
Mulliken charge population of orthorhombic $BiGaO_3$

Species	s	p	d	Total	Charge (electron)
Bi	1.71	1.67	0.00	3.38	1.62
Ga	0.78	1.07	9.99	11.84	1.16
O(1)	1.87	5.06	0.00	6.92	−0.92
O(2)	1.87	5.07	0.00	6.93	−0.93

3.3. Optical properties

Based on the electronic structure, the dielectric function of $BiGaO_3$ was calculated. The $\varepsilon_2(\omega)$ and $\varepsilon_1(\omega)$ as a function of the photon energy are shown in Fig. 4. We only considered the case of the incident radiation with the linear polarization along the [1 1 0] direction. The imaginary part $\varepsilon_2(\omega)$ of the dielectric function is directly connected with the energy band structure. Peaks A (5.56 eV), B (6.61 eV), and C (8.38 eV) correspond to the transition from O 2p VB to Bi 6p CB. Peaks D (11.18 eV) and E (13.36 eV) correspond to the transition from O 2p VB to Ga 4s CB, and peaks F (18.32 eV) and G (20.30 eV) are ascribed to the transition of inner electron excitation from O 2s and Bi 6s levels to CB. It is noted that a peak in $\varepsilon_2(\omega)$ does not correspond to a single interband transition since many direct or indirect transitions may be found in band structure with an energy corresponding to the same peak [19]. The calculated static dielectric constant $\varepsilon_1(0)$ was found to be 9.19.

The calculated results on the absorption spectrum, refractive index, extinction coefficient, reflectivity and energy-loss spectrum are shown in Fig. 5a–e. In our calculation, we used Gaussian smearing that is 0.3 eV. The absorption spectrum started at 2.58 eV and decreased rapidly in the low-energy region. In the range from 0 to 2.58 eV, the reflectivity was lower than 30%, which indicates that $BiGaO_3$ material is transmitting for frequencies <2.58 eV. The calculated reflectivity has a maximum value of roughly 80% at about 25.97 eV. The energy-loss spectrum describes the energy-loss of a fast electron traversing in the material [20]. Its main peak is generally defined as the bulk plasma frequency ω_p, which occurs where $\varepsilon_2 < 1$ and ε_1 reaches the zero point [21]. Moreover, the main peak at about 28.58 eV corresponds to a rapid reduction of the reflectance. This process is associated with the transitions from the filled O 2s and Bi 6s bands to empty CB. The calculated static refractive index is equal to 3.03.

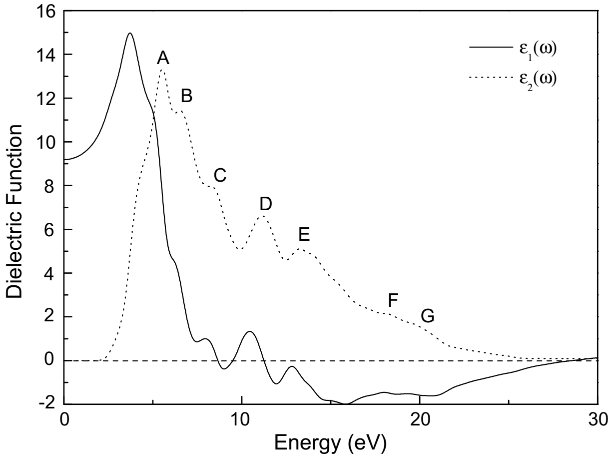

Fig. 4. Calculated imaginary part $\varepsilon_2(\omega)$ and real part $\varepsilon_1(\omega)$ of the dielectric function $\varepsilon(\omega)$ for orthorhombic $BiGaO_3$.

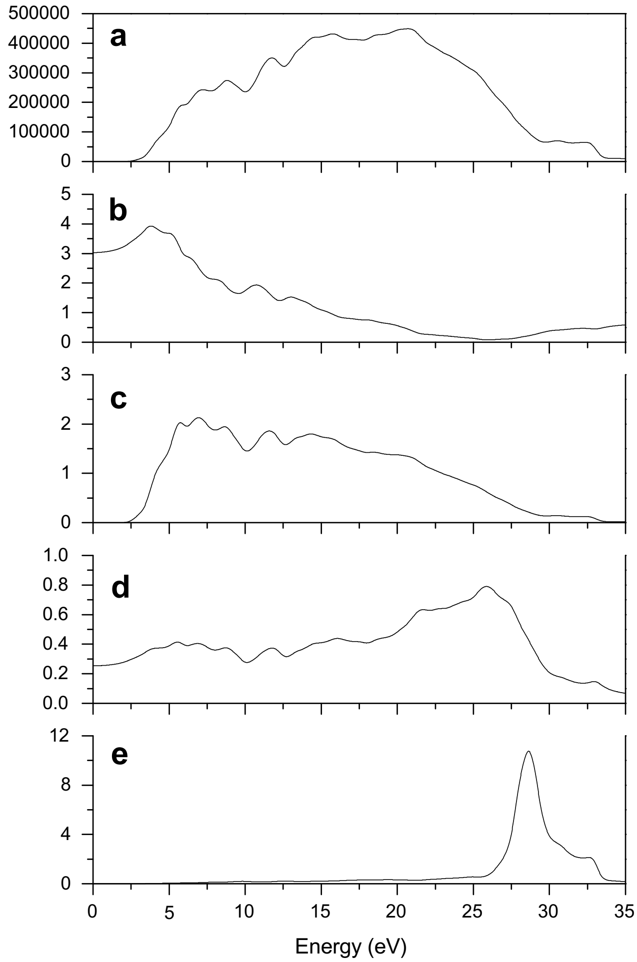

Fig. 5. Calculated optical constants for orthorhombic $BiGaO_3$. (a) Absorption spectrum, (b) refractive index, (c) extinction coefficient, (d) reflectivity, and (e) energy-loss spectrum.

4. Conclusion

In summary, the structural parameters, elastic constants, electronic structures, and optical properties of $BiGaO_3$ were performed by means of the density functional theory within the GGA. Our structural parameters are in agreement with previous calculation and experimental data. The calculated elastic constants indicated that $BiGaO_3$ is mechanically stable. The electronic structures of $BiGaO_3$ revealed that the top of the valence band and the bottom of the conduction band are decided by O 2p and Bi 6p states, respectively, and that $BiGaO_3$ presented a direct band gap of 2.03 eV. Furthermore, the Ga–O bond possesses a stronger covalent bonding strength than the Bi–O bond. Finally, the dielectric function, absorption spectrum, refractive index, extinction coefficient, reflectivity and energy-loss spectrum were obtained. The relations of the optical properties to the interband transitions were also discussed. In the low-energy region, the origin of the spectral peaks are ascribed to the transitions from O 2p VB to Bi 6p CB or even higher conduction band Ga 4s. In the high-energy region, the peak is ascribed to the transition from O 2s and Bi 6s bands to empty CB. At present, there are not yet any experimental results on the elastic constants, electronic and optical properties for the orthorhombic $BiGaO_3$. Therefore, we hope that our calculated results could serve as a reference for future experimental study and develop the optical applications of $BiGaO_3$.

Acknowledgements

This work was supported by the National Natural Science Foundation of China (10572155, 10172030, 50232030) and the Science Foundation of Guangdong Province (2005A10602002).

References

[1] R.E. Eitel, S.J. Zhang, T.R. Shrout, C.A. Randall, I. Levin, J. Appl. Phys. 96 (2004) 2828.

[2] S.J. Zhang, C.A. Randall, T.R. Shrout, Appl. Phys. Lett. 83 (2003) 3150.

[3] J.R. Cheng, W.Y. Zhu, N. Li, L.E. Cross, Mater. Lett. 57 (2003) 2090.

[4] Y. Inaguma, A. Miyaguchi, M. Yoshida, T. Katsumata, Y. Shimojo, R.P. Wang, T. Sekiya, J. Appl. Phys. 95 (2004) 231.

[5] S.V. Halilov, M. Fornari, D.J. Singh, Phys. Rev. B 69 (2004) 174107.

[6] R.E. Eitel, C.A. Randall, T.R. Shrout, P.W. Rehrig, W. Hackenberger, S.-E. Park, Jpn. J. Appl. Phys. 40 (2001) 5999.

[7] J. Iniguez, D. Vanderbilt, L. Bellaiche, Phys. Rev. B 67 (2003) 224107.

[8] P. Baetting, C.F. Schelle, R. LeSar, U.V. Waghmare, N.A. Spaldin, Chem. Mater. 17 (2005) 1376.

[9] A.A. Belik, T. Wuernisha, T. Kamiyama, K. Mori, M. Maie, T. Nagai, Y. Matsui, E. Takayama-Muromachi, Chem. Mater. 18 (2006) 133.

[10] H. Wang, B. Wang, R. Wang, Q.K. Li, Physica B 390 (2007) 96.

[11] H. Wang, B. Wang, Q.K. Li, Z.Y. Zhu, R. Wang, C.H. Woo, Phys. Rev. B 75 (2007) 245209.

[12] P. Ravindran, L. Fast, P.A. Korzhavyi, B. Johansson, J. Appl. Phys. 84 (1998) 4891.

[13] D. Vanderbilt, Phys. Rev. B 41 (1990) 7892.

[14] J.P. Perdew, K. Burke, M. Ernzerhof, Phys. Rev. Lett. 77 (1996) 3865.

[15] M.D. Segall, C.J. Pickard, R. Shah, M.C. Payne, Phys. Rev. B 54 (1996) 16317.

[16] H.J. Monkhorst, J.D. Pack, Phys. Rev. B 13 (1976) 5188.

[17] S. Saha, T.P. Sinha, Phys. Rev. B 62 (2000) 8828.

[18] Z.J. Wu, X.F. Hao, X.J. Liu, J. Meng, Phys. Rev. B 75 (2007) 054115.

[19] M.Q. Cai, Z. Yin, M.S. Zhang, Appl. Phys. Lett. 83 (2003) 14.

[20] A. Bouhemadou, R. Khenata, Comput. Mater. Sci. 39 (2007) 803.

[21] R. Saniz, L.H. Ye, T. Shishidou, A.J. Freeman, Phys. Rev. B 74 (2006) 014209.